AMERICAN SOCIETY FOR MICROBIOLOGY | Journal of Bacteriology®

MEETING PRESENTATION

Esx Paralogs Are Functionally Equivalent to ESX-1 Proteins but Are Dispensable for Virulence in *Mycobacterium marinum*

Rachel E. Bosserman,[a]* Cristal Reyna Thompson,[a] Kathleen R. Nicholson,[a] Patricia A. Champion[a]

[a]Department of Biological Sciences, University of Notre Dame, Notre Dame, Indiana, USA

ABSTRACT *Mycobacterium marinum* is a nontuberculous pathogen of poikilothermic fish and an opportunistic human pathogen. Like tuberculous mycobacteria, the *M. marinum* M strain requires the ESX-1 (ESAT-6 system 1) secretion system for virulence in host cells. EsxB and EsxA, two major virulence factors exported by the ESX-1 system, are encoded by the *esxBA* genes within the ESX-1 locus. Deletion of the *esxBA* genes abrogates ESX-1 export and attenuates *M. marinum* in *ex vivo* and *in vivo* models of infection. Interestingly, there are several duplications of the *esxB* and *esxA* genes (*esxB_1*, *esxB_2*, *esxA_1*, *esxA_2*, and *esxA_3*) in the *M. marinum* M genome located outside the ESX-1 locus. We sought to understand if this region, known as ESX-6, contributes to ESX-1-mediated virulence. We found that deletion of the *esxB_1* gene alone or the entire ESX-6 locus did not impact ESX-1 export or function, supporting the idea that the *esxBA* genes present at the ESX-1 locus are the primary contributors to ESX-1-mediated virulence. Nevertheless, overexpression of the *esxB_1* locus complemented ESX-1 function in the Δ*esxBA* strain, signifying that the two loci are functionally equivalent. Our findings raise questions about why duplicate versions of the *esxBA* genes are maintained in the *M. marinum* M genome and how these proteins, which are functionally equivalent to virulence factors, contribute to mycobacterial biology.

IMPORTANCE *Mycobacterium tuberculosis* is the causative agent of the human disease tuberculosis (TB). There are 10.4 million cases and 1.7 million TB-associated deaths annually, making TB a leading cause of death globally. Nontuberculous mycobacteria (NTM) cause chronic human infections that are acquired from the environment. Despite differences in disease etiology, both tuberculous and NTM pathogens use the ESX-1 secretion system to cause disease. The nontubercular mycobacterial species, *Mycobacterium marinum*, has additional copies of specific ESX-1 genes. Our findings demonstrate that the duplicated genes do not contribute to virulence but can substitute for virulence factors in *M. marinum*. These findings suggest that the duplicated genes may play a specific role in NTM biology.

KEYWORDS ESX-1, ESX-6, mycobacteria, CFP-10, duplication, type VII secretion, gene duplication

Mycobacterium marinum is a nontuberculous mycobacterial pathogen of fresh and salt water ectotherms (1, 2). As with other nontuberculous mycobacteria (NTMs), *M. marinum* is an opportunistic human pathogen that can be contracted from the environment (3, 4). *Mycobacterium tuberculosis* (*M. tuberculosis*) is an obligate human pathogen that causes the human disease tuberculosis (5). Although *M. marinum* differs from *M. tuberculosis*, the two pathogens share virulence pathways that promote survival within the host. As such, *M. marinum* is a well-established and accepted model for several aspects of *M. tuberculosis* pathogenesis (recently reviewed in reference 6).

Up to five ESX systems, ESX-1 through ESX-5, can be encoded within the mycobacterial genome. At least three of these systems (ESX-1, ESX-3, and ESX-5) transport

Received 1 December 2017 **Accepted** 11 March 2018

Accepted manuscript posted online 19 March 2018

Citation Bosserman RE, Thompson CR, Nicholson KR, Champion PA. 2018. Esx paralogs are functionally equivalent to ESX-1 proteins but are dispensable for virulence in *Mycobacterium marinum*. J Bacteriol 200:e00726-17. https://doi.org/10.1128/JB.00726-17.

Editor Victor J. DiRita, Michigan State University

Address correspondence to Patricia A. Champion, pchampio@nd.edu.

* Present address: Rachel E. Bosserman, The University of Texas Health Science Center at Houston, Houston, Texas, USA.

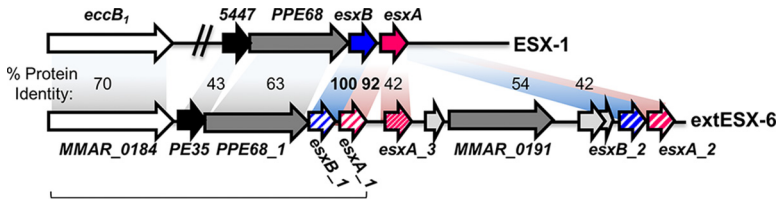

FIG 1 *M. marinum* ESX-6 genes share similarities with ESX-1 genes. Comparison between paralogous genes at the ESX-1 locus and extended ESX-6 locus. The percent identity at the protein level is shown. For simplicity, the entire ESX-1 locus is not depicted; only genes with paralogs in the extended ESX-6 region are shown. The ESX-6 region is bracketed.

protein virulence factors (7–11). The ESX-1 (ESAT-6 system 1) system is required for virulence in both *M. marinum* and *M. tuberculosis* (7, 12). In both species, following bacterial uptake by phagocytic cells, the ESX-1 system damages the phagosomal membrane, resulting in cytosolic access and upregulation of a type I interferon (IFN) response (13–18). Upregulation of the type I interferon response by ESX-1 blocks IFN-γ-mediated killing of *M. marinum*, promoting bacterial survival within the host (19). Importantly, expression of the ESX-1 system from *M. tuberculosis* in ESX-1-deficient *M. marinum* strains restores ESX-1 function, indicating that the two systems are functionally equivalent (20).

All ESX loci encode Esx proteins (WXG100 family proteins) that are approximately 100 amino acids long with a WXG motif (21). EsxA (early secretory antigenic target, 6 kDa [ESAT-6]) and EsxB (culture filtrate protein, 10 kDa [CFP-10]) are WXG100 proteins encoded by the *esxBA* operon at the ESX-1 locus (22, 23). EsxA and EsxB directly interact and form a heterodimer (22–25). EsxA and EsxB promote the assembly of the ESX-1 secretion system and are required for the secretion of other ESX-1 substrates (8, 9, 26–31). EsxA and EsxB are also secreted by the ESX-1 system, indicating that they may perform additional roles in virulence as effector proteins (7–9).

In addition to the *esx* genes located at ESX loci, *M. tuberculosis* and *M. marinum* harbor paralogous *esx* loci elsewhere in the genome, which include PE/PPE genes followed by *esx* genes but not paralogs of genes encoding conserved ESX components (32). PE (proline-glutamate) and PPE (proline-proline-glutamate) family proteins are secreted or associated with the membrane or cell wall (27, 31, 33). Most of the paralogous *esx* loci have not been studied. Recently, studies have shown that the *esxIJ* paralogs and the surrounding genes in *M. tuberculosis* and *M. marinum* (now referred to as ESX-5a) promote the secretion of a subset of ESX-5 substrates (32, 34). These findings indicate that the ESX-5 system is modular and that ESX-5a has an accessory role in protein transport (34).

Although the *M. marinum* and *M. tuberculosis* ESX systems are similar, there are also likely undiscovered differences. In support of this idea, *M. marinum* harbors *esx* paralogs that are not found in *M. tuberculosis* (*MMAR_0184-MMAR_0188*; starting location, bp 218996). This unique locus, designated ESX-6, includes *esx* genes that are similar to the ESX-1 genes, *esxB* and *esxA* (*MMAR_5449* and *MMAR_5450*; starting location, bp 6591158), PE/PPE genes, and a gene paralogous to the conserved component *eccB* (35). The *pe35* and *ppe68_1* genes in the ESX-6 region encode ESX-1 substrates, linking this region to the ESX-1 system (36).

Interestingly, the *esxB* paralog at the ESX-6 locus (*esxB_1*) is predicted to encode a protein that is 100% identical at the amino acid level to the major ESX-1 substrate, EsxB. Because the predicted EsxB_1 protein was identical to EsxB, we took a genetic approach to determine if the ESX-6 region in *M. marinum* was involved in ESX-1-mediated secretion and virulence.

RESULTS

Two genes, which encode identical EsxB proteins, are differentially expressed in *M. marinum*. The *esxB_1* (*MMAR_0187*) gene is in the ESX-6 region (Fig. 1). *esxB_1* is

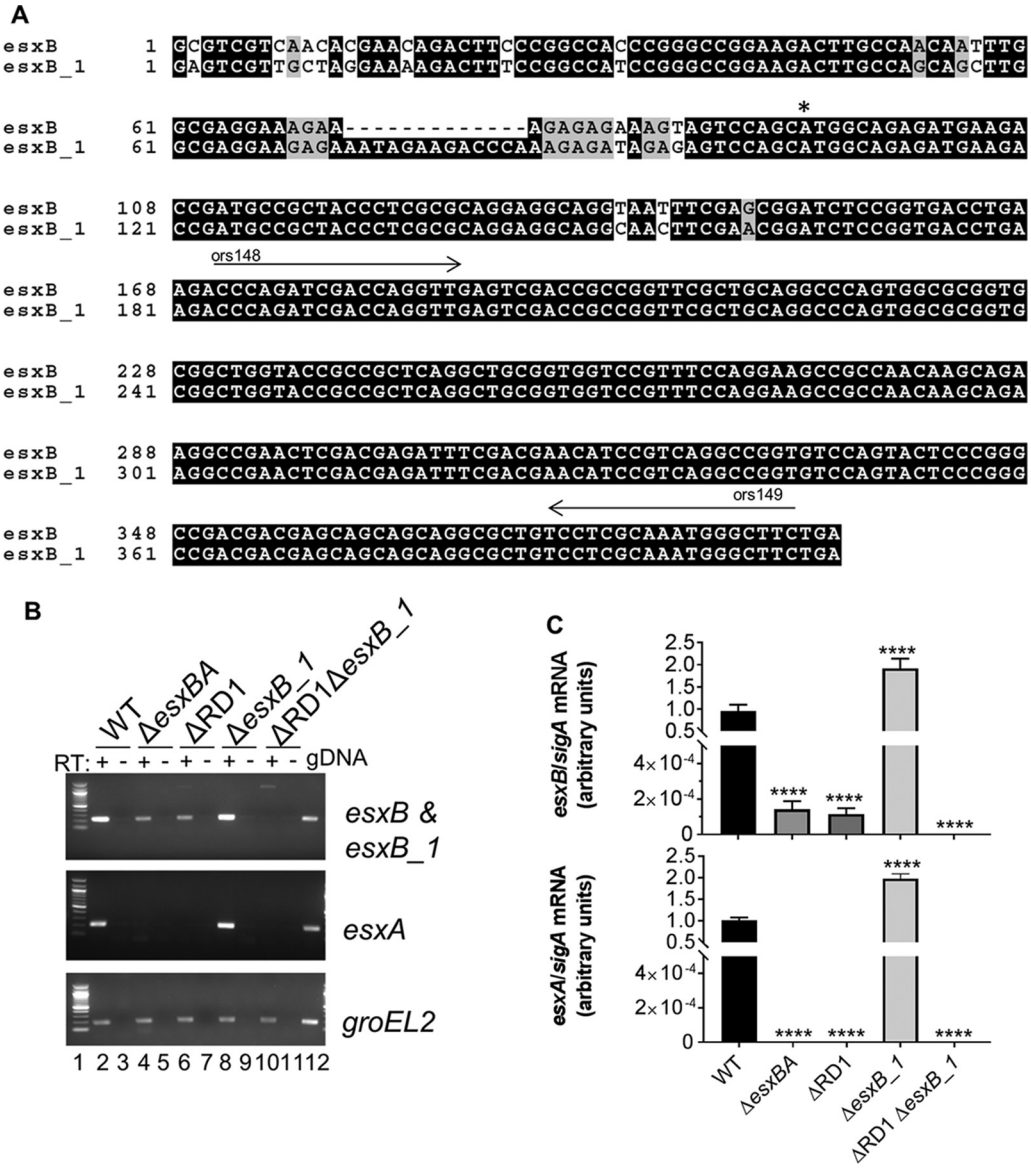

FIG 2 *M. marinum* ESX-6 genes share similarities with ESX-1 genes. (A) Alignment of the *esxB* and *esxB_1* genes from *M. marinum* M. The translational start site is indicated by an asterisk. The arrows indicate the binding sites for ors148 and ors149 primers, which were used for qRT-PCR analysis of the *esxB* and *esxB_1* genes. The alignment was performed using Clustal Omega and visualized using BoxShade. (B) Expression levels of *esxB*, *esxB_1*, and *esxA* were determined using qualitative RT-PCR. RT, reverse transcriptase. The *groEL2* gene transcript was a control for cDNA quality. The no-RT control was a control for contaminating genomic DNA (gDNA). The figure is representative of three independent biological replicates. (C) Expression levels of *esxB*, *esxB_1*, and *esxA* determined using quantitative RT-PCR. *esxB*, *esxB_1*, and *esxA* transcripts were normalized relative to the level of the *sigA* gene. Error bars represent standard deviations of four technical replicates performed on two biological replicates ($n = 8$). Significance relative to the WT strain was determined using a one-way ANOVA ($P < 0.0001$) followed by a Dunnett's multiple-comparison test. (****, $P \leq 0.0001$).

predicted to encode a protein that is 100% identical to EsxB at the amino acid level (Fig. 1). We were interested in understanding if the *esxB_1* gene was expressed in *M. marinum*. We aligned the predicted *esxB* and *esxB_1* coding regions and the upstream intergenic region to establish differences between the two *esxB* genes at the nucleotide level. We found that the *esxB_1* gene was 99% identical to *esxB*, with three synonymous single nucleotide polymorphisms (SNPs) in the predicted open reading frame compared to the sequence of the *esxB* gene (Fig. 2A). Additionally, 11 nucleotides were inserted upstream of the predicted open reading frame of *esxB_1*. From these data, we hypothesized that the *esxB_1* gene would likely have a different expression profile from that of the *esxB* gene.

To determine if the *esxB_1* gene is expressed, we created an *M. marinum* strain bearing an unmarked deletion of the *esxB_1* gene (Δ*esxB_1*). We measured gene expression levels of the *esxB*, *esxB_1*, and *esxA* genes using both qualitative and quantitative reverse transcription-PCR (RT-PCR), as shown in Fig. 2B and C. Because of the close identity between the coding regions of the *esxB* and *esxB_1* genes, our oligonucleotide primers could not distinguish unique transcripts arising from each gene (Fig. 2A). To circumvent this problem, we measured the expression levels of the *esxB* and *esxB_1* genes from the wild-type (WT), Δ*esxBA*, ΔRD1, Δ*esxB_1*, and ΔRD1 Δ*esxB_1* strains under growth conditions that support ESX-1-mediated secretion *in vitro*. We reasoned that *esxB* transcript detected in the WT *M. marinum* strain would represent expression from both the *esxB* and *esxB_1* genes. The ΔRD1 strain bears a deletion that includes the *esxB* and *esxA* genes (7, 12). Therefore, *esxB* transcript detected in the ΔRD1 and Δ*esxBA* strains would represent expression solely from the *esxB_1* gene. Conversely, *esxB* transcript detected in the Δ*esxB_1* strain would represent expression solely from the *esxB* gene. Neither gene is present in the ΔRD1 Δ*esxB_1* strain, which should serve as a control for specificity. The extended ESX-6 locus includes three *esxA* paralogs, the *esxA_1*, *esxA_2*, and *esxA_3* genes (Fig. 1). Because the *esxA* paralogs are divergent from the *esxA* gene (*esxA_1*, 94.1% identity; *esxA_2*, 59.7% identity; *esxA_3*, 59.3% identity), we were able to specifically detect transcript from the *esxA* gene.

As shown in Fig. 2B and C, *esxB* and *esxA* transcripts were detected in the WT strain, as expected (Fig. 2B, lane 2, and C). In strains lacking the *esxB* and *esxA* genes (Δ*esxBA* and ΔRD1 strains), the *esxA* transcript was not detected (Fig. 2B, lanes 4 and 6, and C). In contrast, we observed significantly reduced (levels 3×10^3- to 4×10^3-fold lower than WT levels; $P \leq 0.0001$) but measurable levels of *esxB_1* transcript. The levels of *esxB* and *esxA* transcripts in strains lacking the *esxB_1* gene were significantly increased (~2-fold higher; $P \leq 0.0001$) (Fig. 2C) than levels in the WT strain (Fig. 2B, lane 8, and C). No *esxB* or *esxB_1* or *esxA* transcripts were observed in the ΔRD1 Δ*esxB_1* strain (Fig. 2B, lane 10, and C).

The *groEL2* gene transcript was detected in all strains, serving as a control for cDNA quality (Fig. 2B). No transcripts were detected in the lanes lacking reverse transcriptase, indicating the absence of contaminating genomic DNA.

From these data, we conclude that the *esxB_1* gene is expressed in *M. marinum* M at a low level under the conditions tested. Accordingly, the *esxB* and *esxB_1* gene transcripts detected in the WT strain are due primarily to *esxB* gene expression.

EsxB_1 and the extended ESX-6 region are dispensable for ESX-1 secretion and function. EsxB and EsxA are required for ESX-1 export and virulence (8, 9). Since the proteins encoded by the *esxB* and *esxB_1* genes, EsxB and EsxB_1, are predicted to be identical, we hypothesized that EsxB_1 and the extended ESX-6 region would be required for ESX-1 export. To test this hypothesis, we examined ESX-1 secretion and function in the absence of the *esxB_1* gene or the ESX-6 region.

We measured ESX-1 protein secretion directly into the culture medium during *in vitro* growth of the bacteria. The WT strain produced EsxB and EsxA and secreted both proteins into the culture supernatant (Fig. 3A, lanes 1 and 2). EsxB and EsxA proteins were not detected in the cell lysate or culture supernatant fractions from the Δ*esxBA* strain (Fig. 3A, lanes 3 and 4). The Δ*esxB_1* strain and the Δ*esxB_1* strain expressing *esxB_1-esxA_3* from an integrating plasmid (Δ*esxB_1* complemented strain) also produced and secreted EsxB and EsxA (Fig. 3A, lanes 5 to 8).

WT *M. marinum* lyses sheep red blood cells (sRBCs) in a contact-dependent, ESX-1-dependent manner (20, 37, 38). We examined hemolytic activity of the WT, Δ*esxB_1*, and complemented strains as a reporter of ESX-1 function. The WT strain lysed sRBCs at a level similar to that of the positive control, distilled H_2O (dH_2O) (Fig. 3B). The ΔRD1 strain, which lacks ESX-1 secretion, exhibited significantly reduced hemolytic activity compared to that of the WT strain ($P < 0.0001$ compared to results with the WT strain). The ΔRD1 Δ*esxB_1* strain also displayed significantly reduced hemolytic activity ($P < 0.0001$ compared to results with the WT strain). The Δ*esxB_1* strain lysed sRBCs to levels

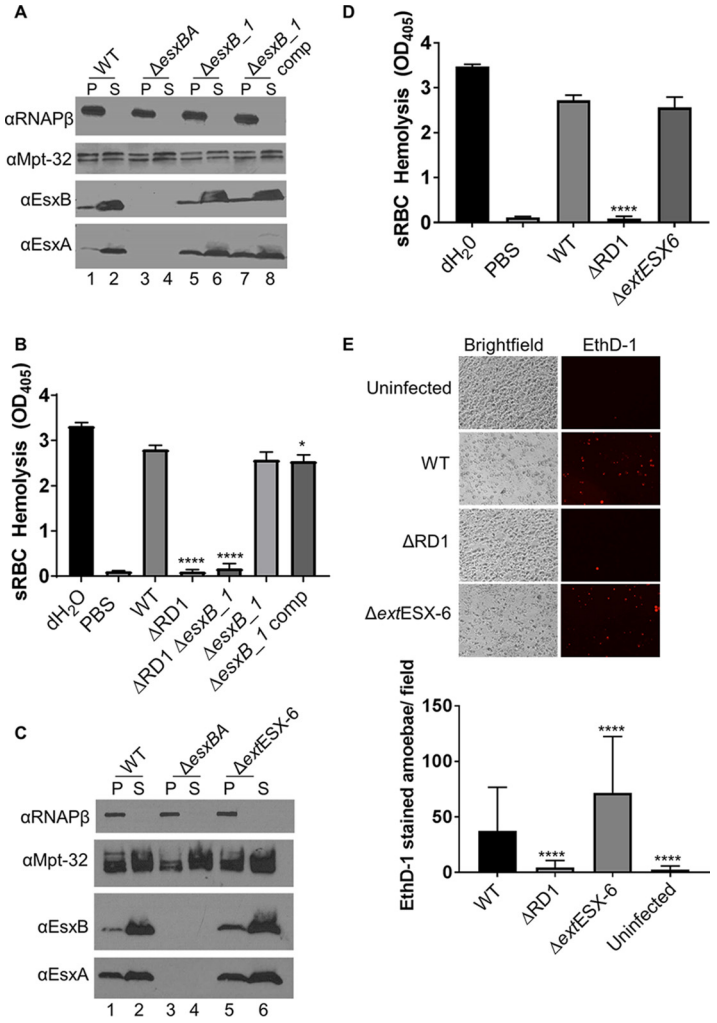

FIG 3 The *esxB_1* gene and the extended ESX-6 region are dispensable for ESX-1 secretion and activity. (A) ESX-1 secretion assay. The cytosolic protein RNA polymerase subunit beta (RNAP-β) was a lysis control for supernatant fractions. Mpt-32, a Sec-secreted protein, served as a loading control. P, pellet, S, supernatant; comp, the Δ*esxB_1*/p_{Mops}*esxB_1-esxA_3* complementation strain (Mops is the mycobacterial optimal promoter). (B) Sheep RBC hemolysis assay. The data represent at least four biological replicates, each with three technical replicates. The data were averaged, and the propagated error was calculated from the standard deviation from each replicate. The error bars represent the propagated error. Significance was calculated using an ordinary one-way ANOVA ($P < 0.0001$) followed by a Sidak's multiple-comparison test between all possible pairs. Significance relative to results with the WT are indicated (****, $P < 0.0001$; *, $P = 0.0269$). Note that there was no significant difference between results for the *esxB_1* and *esxB_1* and complemented strains. (C and D) ESX-1 secretion assay and sRBC hemolysis assay. The ΔextESX-6 strain includes deletion of the *MMAR_0184-esxA_2* genes. The data from at least four biological replicates were averaged, and the propagated error was calculated from the standard deviation from each replicate. The error bars represent the propagated error. Significance was calculated using an ordinary one-way ANOVA ($P < 0.0001$) followed by Tukey's multiple-comparison test between all possible pairs. Significance relative to results with the WT strain is shown (****, $P = 0.0001$). (E) Infection of *A. castellanii* with *M. marinum*. Each infection was performed in technical duplicate on three biological replicates. Representative images are shown above. All images in the figure were adjusted with +40% brightness to aid in visualization. The ethidium homodimer-1-stained amoebae were quantified using ImageJ. All fields from three infections were averaged. The error bars represent the standard deviation between fields ($n = 20$). Significance was determined using an ordinary one-way ANOVA ($P < 0.0001$) followed by Dunnett's multiple-comparison test relative to results with the WT strain (****, $P = 0.0001$).

not significantly different from the level of the WT strain. The *esxB_1* complemented strain exhibited a slight but significant reduction in hemolysis compared to that of the WT strain ($P = 0.0269$). Because there was no significant difference between levels of hemolysis in the WT and the Δ*esxB_1* strains, we conclude that the *esxB_1* gene is not

required for ESX-1-mediated hemolysis. Moreover, overexpression of the *esxB_1-esxA_3* genes does not seem to affect the production and secretion of EsxA and EsxB when the *esxBA* genes are present.

We created a strain bearing a deletion of the extended ESX-6 region, encompassing genes *MMAR_0184-esxA_2* (ΔextESX-6) and tested the ΔextESX-6 strain for ESX-1 secretion and hemolysis. Similar to findings with the Δ*esxB_1* strain, we observed no changes in the secretion of EsxA and EsxB in the ΔextESX-6 strain (Fig. 3C, lanes 5 and 6). The ΔextESX-6 strain retained hemolytic activity that was not significantly different from that of the WT strain (Fig. 3D). From these data, we conclude that the *esxB_1* gene and the extended ESX-6 region are dispensable for both hemolysis and ESX-1-mediated export of EsxB and EsxA *in vitro*.

The ESX-1 system in *M. marinum* is required for cytotoxicity in cellular models of infection including RAW 264.7 murine macrophage-like cells and amoebae (39, 40). To test ESX-1-mediated cytotoxicity, we infected amoebae at a multiplicity of infection (MOI) of 10 with the WT, ΔRD1, and ΔextESX-6 strains and stained the amoebae monolayer with ethidium homodimer (EthD-1). EthD-1 is a nucleic acid stain that is not membrane permeable. Therefore, only permeabilized cells stain with EthD-1. We quantified the cytotoxicity of each strain by counting EthD-1-stained cells (38, 41). As shown previously, infection with the WT strain led to cytolysis of the amoebae. Infection with the ΔRD1 strain resulted in a significant decrease in cytolysis of the amoebae (Fig. 3E) ($P = 0.0001$). Consistent with our findings shown in Fig. 3A to D, the ΔextESX-6 strain exhibited cytotoxicity against amoebae, with a significantly greater number of stained cells than in the WT strain ($P = 0.0001$). Likewise, we found that the Δ*esxB_1* strain caused cytolysis of RAW 264.7 cells (see Fig. S1 in the supplemental material). Together, these findings indicate that the *esxB_1* gene and the extended ESX-6 region are not required for ESX-1 secretion or virulence.

The EsxB_1 and EsxA_1 proteins encoded by ESX-6 can be secreted through ESX-1 and can promote ESX-1 activity. We previously observed the EsxB_1 protein in secreted protein fractions generated from the ΔRD1 *M. marinum* strain using proteomics (42). However, we have not detected EsxB_1 in *esxB*-deficient strains by Western blot analysis, despite the fact that EsxB antibody should recognize EsxB_1 (Fig. 3A, lanes 3 and 4). Based on the low level of expression of the *esxB_1* gene (Fig. 2B and C), we suspect that the levels of EsxB_1 produced by *M. marinum* are below the limits of detection by Western blot analysis (41, 43–45).

We hypothesized that we could detect the EsxB_1 and EsxA_1 proteins when the *esxB_1-esxA_3* genes were constitutively expressed from an exogenous promoter. While the epitope recognized by the EsxA antibody is conserved in the EsxA_1 protein (12/13 residues), it is not well conserved in the EsxA_3 protein (5/13 conserved residues). Therefore, while it is likely that the EsxA antibody primarily detects the EsxA_1 protein, we cannot rule out that it may also detect the EsxA_3 protein. To this end, we introduced the *esxB_1-esxA_3* expression plasmid into the Δ*esxBA* deletion strain. As shown in Fig. 4, the WT strain produced and secreted EsxB and EsxA (Fig. 4A, lanes 1 and 2). No EsxA or EsxB protein was detected in the Δ*esxBA* deletion strain (Fig. 4A, lanes 3 and 4). Expression of *esxB_1-esxA_3* from a constitutive promoter resulted in the production and secretion of the EsxB_1 and EsxA_1/EsxA_3 proteins from the Δ*esxBA* strain (Fig. 4, lanes 5 and 6). These data demonstrate that EsxB_1 and EsxA_1/EsxA_3 can be secreted by *M. marinum* during growth *in vitro*.

We next sought to determine if the EsxB_1 and EsxA_1/EsxA_3 proteins were secreted by the ESX-1 secretion system. Because EsxB_1 is identical to EsxB, we hypothesized that the EsxB_1 protein was competent for secretion through the ESX-1 system.

It is well established that the ESX-1 systems in *M. marinum* and in *M. tuberculosis* are functionally equivalent (14, 15, 17, 18, 20). As such, *M. tuberculosis* genes can cross-complement *M. marinum* strains bearing deletions in ESX-1 genes (20). In *M. tuberculosis* the last 7 amino acids of EsxB are necessary and sufficient for recognition by the ESX-1 system (26, 28). We first confirmed that the EsxB protein from *M. tuberculosis*

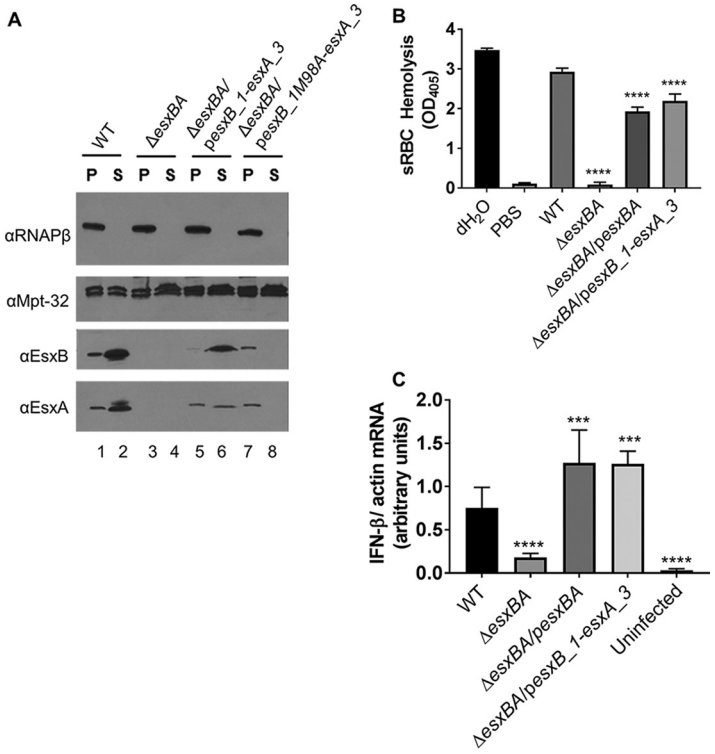

FIG 4 EsxB_1 and EsxA_1 can by secreted by Esx-1 and are functionally redundant. (A) ESX-1 secretion assay. Controls for the secretion assay are the same as those described in the legend to Fig. 2. In this assay, the EsxB and EsxA antibodies are recognizing EsxB_1 and EsxA_1/EsxA_3 for lanes 5 to 8. Data are representative of at least three biological replicates. (B) sRBC hemolysis assay. The data represent at least four biological replicates, each with three technical replicates. The data were averaged, and the propagated error was calculated from the standard deviation from each replicate. The error bars represent the propagated error. Significance was calculated using an ordinary one-way ANOVA ($P < 0.0001$) followed by Dunnett's multiple comparison for results compared to those with the WT strain (****, $P < 0.0001$). (C) qRT-PCR analysis measuring IFN-β expression normalized to actin expression at 24 h postinfection with *M. marinum*. The data are the average of four biological replicates, each with two technical replicates. The error bars represent the propagated error ($n = 8$ total). Statistical significance was determined using an ordinary one-way ANOVA ($P < 0.0001$) followed by Dunnett's multiple-comparison test comparing results with infection by the WT strain. (****, $P = 0.0001$; ***, $P = 0.0003$ and 0.0002 for p*esxBA* and p*esxB_1-esxA_3*, respectively).

($EsxB_{MT}$) was recognized by the *M. marinum* ESX-1 system through its C terminus. We confirmed that $EsxA_{MT}$ and $EsxB_{MT}$ were produced and secreted from *M. marinum* (Fig. S2A and B). We demonstrated that $EsxB_{MT}$ proteins bearing point mutations in residues required for ESX-1 recognition were also required for export in *M. marinum* (Fig. S2A and B). For example, an $EsxB_{MT}$ mutant protein with the M at position 98 changed to an A (EsxBM98A_{MT}) was produced in but not secreted from WT *M. marinum* (Fig. S2B). Together, these data show that $EsxB_{MT}$ proteins with mutations in residues required for ESX-1 recognition were also not secreted by *M. marinum*.

To determine if the EsxB_1 and EsxA_1 proteins are targeted for ESX-1 export similarly to the EsxB and EsxA proteins, we mutagenized the *esxB_1* gene such that it would produce an EsxB_1M98A protein. If EsxB_1 is secreted by the ESX-1 system, the EsxB_1M98A protein should not be secreted. Interestingly, in the Δ*esxBA* strain expressing the mutagenized *esxB_1* M98A allele, the proteins EsxB_1M98A and EsxA_1 were produced but no longer secreted into the culture supernatant (Fig. 4A, lanes 7 and 8). These data suggest that secretion of EsxB_1 and EsxA_1 occurs in an ESX-1-dependent fashion, as the M98 residue is required for targeting $EsxB_{MT}$ to ESX-1 in *M. marinum* (Fig. S2B). Collectively, these data indicate that EsxB_1 and EsxA_1 can be secreted by the ESX-1 system in *M. marinum*.

Because the EsxB_1 and EsxA_1 or EsxA_3 proteins were secreted by the ESX-1 system, we tested if they were functionally equivalent to the EsxA and EsxB proteins

encoded by the ESX-1 system. We first assessed ESX-1-mediated hemolysis. As shown previously, the WT strain displayed hemolytic activity. Hemolysis was reduced in the Δ*esxBA* strain and restored, although not completely, by expression of the *esxBA* or the *esxB_1-esxA_3* genes (Δ*esxBA*/p*esxB_1-esxA_3* strain) (Fig. 4B).

The *esxB_2* and *esxA_2* genes in the extended ESX-6 locus encode additional paralogs that are 54% and 42% identical, respectively, to the EsxB and EsxA proteins encoded by the ESX-1 locus (Fig. 1; see also Fig. S3A in the supplemental material). We performed the same experiment expressing the *esxB_2 esxA_2* genes in the Δ*esxBA* strain. Expression of the *esxB_2-esxA_2* genes did not restore hemolytic activity to the Δ*esxBA* strain (Fig. S3B). Together, these data indicate that the *esxB_1-esxA_3* genes, but not the *esxB_2-esxA_2* genes, can functionally complement ESX-1-mediated hemolysis.

In the host cell infection models, ESX-1-mediated phagosomal lysis is required to elicit induction of the cytokine IFN-β (13) and to promote host cell cytotoxicity (14, 15, 46, 47). We next tested if constitutive expression of the *esxB_1-esxA_3* genes could restore the IFN-β response to the attenuated Δ*esxBA* strain. IFN-β transcription was measured using quantitative RT-PCR. As shown in Fig. 4C, IFN-β mRNA was induced by the WT *M. marinum* strain. In contrast, the Δ*esxBA* strain failed to induce expression of IFN-β ($P = 0.0048$ compared to results with the WT strain), similar to the uninfected macrophage cells ($P = 0.0001$ compared to results with the WT strain). Induction of IFN-β expression was restored by the expression of the *esxBA* genes ($P = 0.0003$ compared to results with the WT strain) or the *esxB_1-esxA_3* genes (Δ*esxBA*/p_{Mops}*esxB_1-esxA_3*; $P = 0.0002$ compared to results with the WT strain) in the Δ*esxBA* strain (Fig. 4C). Together these data demonstrate that the *esxB_1* locus, when overexpressed under a constitutive promoter, can restore ESX-1-dependent cytolysis and induction of IFN-β in macrophage-like cells.

DISCUSSION

In this study, we examined the role of the ESX-6 region of *M. marinum* in ESX-1 protein secretion. Our major conclusions were that, although the *esxB_1* gene and the extended *ESX-6* locus had no discernible impact on ESX-1 secretion or cytotoxicity under the conditions examined, the Esx proteins at the ESX-6 locus could functionally substitute for the EsxA and EsxB virulence factors encoded at the ESX-1 locus. This conclusion is based upon the following evidence. First, we found that the *esxB_1* gene was expressed in *M. marinum* to levels below the level of the *esxB* gene at the ESX-1 locus. Second, deletion of the *esxB_1* gene or deletion of the extended ESX-6 locus did not lead to appreciable changes in ESX-1-mediated activities, including secretion, hemolysis, and cytolysis of host cells. Third, in the absence of the *esxBA* genes present at the ESX-1 locus, we found constitutive expression of the Esx genes at the ESX-6 locus resulted in secretion of EsxB_1 and EsxA_1 in an ESX-1-dependent manner. Constitutive expression of these genes also restored both hemolysis and induction of the type I IFN response during macrophage infection. Together, our experimental findings support the idea that the Esx genes in the ESX-6 region can functionally compensate for genes at the ESX-1 locus when they are expressed at higher levels. Our findings are consistent with those from previously published work. We previously reported the detection of a secreted EsxB protein in strains lacking the *esxB* gene from the ESX-1 locus using proteomics (27, 41, 48). Based on our findings, we were observing the secretion of EsxB_1 onto the *M. marinum* cell surface and into the culture supernatant. We previously identified EsxB_1 in secreted protein fractions using proteomics in the absence of the ESX-1 system (27, 48); when these earlier results are considered with our findings here, our findings indicate that EsxB_1 protein can be secreted by ESX-1-dependent and ESX-1-independent mechanisms. The idea that ESX-1-associated proteins can be secreted independently of ESX-1 in mycobacteria has been suggested previously (49).

The extended ESX-6 region is 99% identical at the nucleotide level in the *M. marinum* E11 and M strains. It was suggested previously by Weerdenburg et al. that *M. marinum* has a wide arsenal of host-specific virulence determinants. Using transposon-directed insertion site sequencing (TraDIS), they found that the ESX-6 locus in *M.*

marinum E11, a fish-derived *M. marinum* strain, was specifically required for infection of the fish cell line CLC (carp leukocyte cell line) and not required for virulence in amoebae or RAW 264.7 cells (50). Our findings are consistent with those by Weerdenburg et al. and build on these studies that show that the Esx paralogs at the ESX-6 locus can indeed be secreted by the ESX-1 system and can promote virulence in RAW 264.7 cells. Consistent with the idea that the ESX-6 region may be a host-specific locus, some of the genes in the extended ESX-6 region are also present in the frog pathogen *Mycobacteria ulcerans* ecovar Liflandii and in the human isolate *M. ulcerans* subsp. *shinshuense* (see Fig. S4 in the supplemental material) (35, 50, 51). *M. ulcerans* and *M. marinum* are closely related and genetically similar (52, 53). In contrast, the ESX-6 region is not found in *M. tuberculosis*, whose host range is restricted to humans.

Our findings shed light on the requirement of two ESX-1 substrates for secretion and virulence. The PE35 and PPE68_1 proteins, encoded by genes at the ESX-6 locus, have previously been shown to be secreted by the ESX-1 system in *M. marinum* (36, 54, 55). Our findings using the extended ESX-6 deletion strain indicate that these substrates are dispensable for ESX-1 function and for virulence in amoebae and macrophages.

Here, we sought to define the contribution of the EsxB_1 to ESX-1-mediated secretion and virulence because the EsxB_1 protein is identical to the EsxB virulence factor. Although we have measured the secretion of the EsxB_1 protein using proteomics (27, 48), we did not detect EsxB_1 protein in our strains by Western blot analysis. We suspect that this is because the levels of EsxB_1 protein expressed by *M. marinum* are below the limit of detection for Western blot analysis at the concentration of protein loaded. Indeed, our analysis of *esxB_1* gene expression indicates that the *esxB* and *esxB_1* genes are differentially expressed. One possible explanation for the difference in the levels of *esxB* and *esxB_1* gene expression is a repositioning of the transcriptional start site, also called transcriptional start site turnover. This was recently described with the *pelE* and *pelD* paralogs of the phytopathogenic bacteria *Dickeya* (56). Moreover, the promoter sequences differ between the two genes. Consistent with these findings, the levels of *esxB_1* gene expression are insufficient to substitute for the loss of the *esxBA* genes at the ESX-1 locus. However, increasing the expression of the *esxB_1 esxA_1* and *esxA_3* genes using a synthetic promoter allowed the ESX-6 proteins to specifically substitute for *esxBA*. One possibility is that under different environmental conditions, the expression of the genes at the ESX-6 locus could be upregulated via an unknown mechanism.

One caveat to this study is that we measured *esxB_1* gene expression in the absence of the *esxB* gene and, therefore, in the absence of a functional ESX-1 system. Consequently, if having a functional ESX-1 system has any influence on ESX-6 gene expression, we may have missed that relationship in this study. However, we did observe a 2-fold increase in *esxB* and *esxA* gene expression levels in the absence of the *esxB_1* gene. Likewise, we recently reported that expression of the *esxA_1* gene is downregulated in the absence of a functional ESX-1 system (57). Therefore, there may be an as of yet undiscovered regulatory mechanism that links the expression of the ESX-1 and ESX-6 loci.

The ESX-6 region is organized in the genome similarly to the accessory ESX system, ESX-5a (34). ESX-5a is located apart from the ESX-5 region in *M. marinum* as well as in *M. tuberculosis*. In accessory systems, the *esx* gene duplications are often preceded by a PE/PPE gene pair (32). Likewise, in the ESX-6 region, *esxB_1* and *esxA_1* are preceded by *pe35* (*MMAR_0185*) and *ppe68_1* (*MMAR_0186*). Interestingly, the ESX-6 region has already been linked to ESX-1 secretion. However, our data do not support the idea that the ESX-6 region serves a purpose similar to that of the ESX-5a region. Indeed, most of the ESX-1 substrates are required for ESX-1 secretion or virulence (8, 9, 29–31, 58). We found that deletion of the extended ESX-6 region did not impact secretion of the major ESX-1 substrates, EsxA and EsxB, or virulence.

Finally, the duplication of the *esxBA* genes at the ESX-6 locus is not unique in *M. marinum*. For example, the EsxN protein is a substrate of the ESX-5 system (59). There are seven EsxN paralogs in the *M. marinum* M genome, four (EsxN, EsxN_1, EsxN_2

[Esx5a locus], and EsxN_3) of which are identical at the amino acid level, much like EsxB and EsxB_1 (60). *M. tuberculosis* has four EsxN paralogs, but they are not identical at the amino acid level, drawing a distinction between the two pathogens. It would be interesting to determine if the *esxN* genes are differentially expressed and if these proteins can functionally substitute for the EsxN protein encoded at the ESX-5 locus. Together, our data indicate that *M. marinum* maintains paralogous Esx genes which, when expressed without regulation, can functionally substitute for known virulence factors.

MATERIALS AND METHODS

Growth of mycobacterial strains. All *M. marinum* strains used in this study are derived from the *M. marinum* M strain (ATCC BAA-535) and are listed in Table S1 in the supplemental material. *M. marinum* strains were maintained at 30°C in Middlebrook 7H9 liquid broth (Sigma-Aldrich, St. Louis, MO) with 0.5% glycerol and 0.1% Tween 80 (Amresco, Solon, OH) in the presence of kanamycin (20 μg/ml; IBI Scientific, Peosta, IA) or hygromycin (50 μg/ml; EMD Millipore, Billerica, MA), where appropriate. For calculations regarding the number of bacterial cells, it was estimated that 1 unit of optical density unit at 600 nm (OD_{600}) is 7.7×10^7 cells/ml (61).

Nomenclature was assigned as suggested by Bitter et al. (62). Briefly, Ecc indicates ESX conserved component. Esx, PE, and PPE proteins are named based on their respective protein families. Esp is ESX secretion-associated protein; Esp proteins are region-specific proteins that are not conserved components. Genes are from the *M. marinum* M strain unless annotated otherwise. The subscript MT refers to genes and proteins from *M. tuberculosis* H37Rv. Subscript 1 indicates genes that are in the ESX-1 locus (e.g., $eccB_1$). Duplicate genes are referred to with underscores and 1, 2, or 3 (e.g., *esxB_1*), according to MycoBrowser (60).

Protozoan strains and growth conditions. *Acanthamoeba castellanii* (Douglas) Page was obtained from the American Type Culture Collection (ATCC 30234). Amoebae were grown and maintained in peptone-yeast-glucose (PYG) medium as previously described (40).

Strains and plasmids. All plasmid preparations were performed using an AccuPrep Plasmid Mini extraction kit (Bioneer, Alameda, CA). All oligonucleotide primers were purchased from Integrated DNA Technologies (IDT, Coralville, IA). DNA sequencing was performed at the Genomics and Bioinformatics Core Facility at the University of Notre Dame. All restriction enzymes were purchased from NEB and used according to the manufacturer's instructions. Plasmids were introduced into mycobacterial strains by electroporation (63).

Isolation of *M. marinum* genomic DNA. For all cloning applications, *M. marinum* genomic DNA was isolated as follows (8). Cells from 5 to 10 ml of 7H9 cultures (OD_{600} of $>$2.0) were collected by centrifugation and were resuspended in 450 μl of lysis solution (25 mM Tris-HCl, pH 7.9, 10 mM EDTA, 50 mM glucose) containing 50 μl of lysozyme (Sigma) (10 mg/ml) and incubated overnight at 37°C. One hundred microliters of 10% SDS and 50 μl of proteinase K (10 mg/ml) were added, and samples were then incubated at 55°C for 30 min. Cetrimide (hexadecyltrimethylammonium bromide; 100 mg/ml with 41 mg/ml NaCl [Sigma-Aldrich]) was added, and the samples were incubated for 10 min at 65°C. An equal volume of chloroform (Fisher BioReagents) was added, and the extraction was centrifuged for 5 min at 13,000 rpm. The aqueous layer was collected, and the chloroform extraction was then repeated. DNA from the aqueous layer was precipitated with 0.7 volume of isopropanol (Fisher), incubated for 10 min at room temperature, and then collected by centrifugation at 13,000 rpm for 10 min. The DNA pellet was washed with 70% ethanol, dried, and then dissolved in Tris-EDTA (TE) buffer overnight at 4°C.

For purposes of verifying *M. marinum* strains, a rapid genomic DNA isolation protocol was used. Cells were collected from 1 to 2 ml of *M. marinum* strains grown in 7H9 medium as described above to an OD_{600} of greater than 2.0. The cells were resuspended in 500 μl of phosphate-buffered saline (PBS) and lysed using a Mini-Bead Beater-24 (BioSpec, Bartlesville, OK) as described previously (41). Lysates were clarified, and DNA was extracted as above.

Expression plasmid construction. (i) *esxB_1* expression plasmid. The p_{Mops}*MMAR_esxB_1-esxA_3* plasmid was constructed using the FastCloning method as previously described (64, 65). The *MMAR_0187-MMAR_0189* region was amplified from *M. marinum* M genomic DNA using oligonucleotide primers ors217 (5′-ATTCAGGAGTCCAGCATGGCAGAGATGAAGACCGATG-3′) and ors218 (5′-GCCTGAGCGGTCCCGCTAGGAGAACAGGGTTGCCAG-3′). The p_{Mops}*MMAR_0039* plasmid, excluding the *MMAR_0039* open reading frame, was amplified using oligonucleotide primers omr9 and omr10 (65). The resulting plasmid bears the *esxB_1*, *esxA_1*, and *esxA_3* genes (*MMAR_0187-MMAR_0189*) behind the mycobacterial optimal promoter (MOP) (66). For these and subsequent primer sequences, underscored bases denote extensions that correspond with the amplified vector. The final p_{Mops}*MMAR_esxB_1-esxA_3* plasmid was confirmed by DNA sequencing using the MOPS sequencing primers and the MOPS hygromycin reverse primers described by Reyna et al. (67).

(ii) *esxBA* expression plasmid. The p_{Mops}*MMAR_esxBA* plasmid was constructed and confirmed exactly as described above for the *esxB_1* expression plasmid. The *esxBA* genes were amplified from *M. marinum* genomic DNA using oligonucleotide primers orb38 (5′-ATTCAGGAGTCCAGCATGGCAGAGATGAAGACCGATG-3′) and orb39 (5′-GCCTGAGCGGTCCCGTTAAGCAAACATCCCCGTGAC-3′).

(iii) *esxB_2* expression plasmid. The p_{Mops}*MMAR_esxB_2-esxA_2* plasmid was constructed and confirmed exactly as described above for the *esxB_1* expression plasmid. The *MMAR_0195-MMAR_0196* region was amplified from *M. marinum* genomic DNA using oligonucleotide primers orb66 (5′-ATTCAGGAGTCCAGCATGGCGGAGATGAAGACCGATG-3′) and orb67 (5′-GCCTGAGCGGTCCCGCTAGGCGAACAGGGTTGCCA-3′).

Site-directed mutagenesis. Site-directed mutagenesis was performed as described previously using a QuikChange (Agilent) site-directed mutagenesis approach (26). The *esxB_1* M98A expression plasmid was generated by site-directed mutagenesis using the p_{Mops}*esxB_1-esxA_3* plasmid and oligonucleotide primers M98AF_MM (5′-GCTGTCCTCGCAA**GC**GGGCTTCTGATT-3′) and M98AR_MM (5′-AATCAGAAGCCC **GC**TTGCGAGGACAGC-3′). The primers were designed to mutagenize the 98th codon of the *esxB_1* gene from a methionine codon to an alanine codon (mutagenized bases shown in bold). The mutation was confirmed by DNA sequencing using the MOPS sequencing primers described by Reyna et al. (67).

Site-directed mutagenesis was also performed to introduce mutations in the $esxB_{MT}$ gene on the pMH406H plasmid (26, 48). Oligonucleotide primers described by Champion et al. (26) were used to introduce the S95A, S96A, Q97A, M98A, and F100A mutations in the $esxB_{MT}$ allele. The L94A mutation was introduced using oligonucleotide primers L94A_TBFwd (5′-GCAGCAGCAGGCG**GC**GTCCTCGCAAAT-3′) and L94A_TBRvs (5′-CATTTGCGAGGAC**GC**CGCCTGCTGCTG-3′). The G99A mutation was introduced using oligonucleotide primers G99A_TBFwd (5′-CCTCGCAAATGG**C**CTTCTGACCCGC-3′) and G99A_ TBRvs (5′-GCGGGTCAGAAG**G**CCATTTGCGAGG-3′).

***M. marinum* strain construction. (i) Δ*esxB_1* and ΔRD1 Δ*esxB_1* strains.** To generate an in-frame deletion of the *esxB_1* gene, we used an allelic exchange approach as described previously (65, 68). The 1,446 bp upstream of the *esxB_1* (*MMAR_0187*) gene was amplified from *M. marinum* M ΔRD1 genomic DNA using oligonucleotide primers ors202 (5′-TGGTGTCACGCTCGTCGGCGGGCGCCGATGAAATCTC-3′) and ors80 (5′-TCATGTCGTATTGCTCCGTTTCTTTGTCGTTTTAGGGGAA**CTTAAG**GCTGGACTCTCTATCTCTTTG-3′). The 1,500 bp downstream of the *MMAR_0187* gene was amplified from *M. marinum* ΔRD1 genomic DNA with oligonucleotide primers ors79 (5′-**CTTAAG**TTCCCCTAAAACGACAAAGAAACGGAGCAATACGACA TGAC-3′) and ors203 (5′-GCAGTCAGGCACCGTCAACTCGATGGCTAGCTCATCC-3′). An AflII site (shown in bold) was introduced between the two flanking regions. The upstream and downstream products were joined together by fusion PCR using oligonucleotide primers ors202 and ors203. The p2NIL plasmid (gift from Tanya Parish [plasmid 20188; Addgene]) was amplified using oligonucleotide primers ors116 and ors117 (65). The p2NIL-Δ*esxB_1* plasmid was generated by FastCloning (64), mixing the fusion PCR and the p2NIL PCR products. The plasmid was confirmed by DNA sequencing using oligonucleotide primers pNILFwdPst1 and p2NILRev (65). The pGOAL cassette (from the pGOAL19 plasmid, gift from Tanya Parish [plasmid 20190; Addgene]) was introduced into p2NIL-Δ*esxB_1* exactly as described by Williams et al. (65). Insertion of the pGOAL cassette was confirmed by restriction digest. The p2NIL-Δ*esxB_1* suicide plasmid was introduced into the WT strain and the ΔRD1 strain. Colonies bearing integrated plasmids (merodiploid strains) were selected as previously described (65, 68). Genomic DNA was isolated from white sucrose-resistant colonies. Loss of the *esxB_1* open reading frame was screened by PCR analysis and confirmed by DNA sequencing of the PCR product using oligonucleotide primers ors223 (5′-TGGT GAGAGTCGTTGCTAGG-3′) and ors224 (5′-CTGCACAATGCGGATCACAC-3′).

(ii) ΔextESX-6 (*MMAR_0184-esxA_2*) strain. The region 1,418 bp upstream of the *MMAR_0184* gene was amplified from *M. marinum* genomic DNA using oligonucleotide primers orb90 (5′-TGGTGTCACGC TCGTCCTGTTCGGTAGCGGTAATG-3′) and orb94 (5′-GCTGCTGGTGGGCTAACTCGCCATGTGTCACTCG-3′). The 1,449-bp region downstream of the *esxA_2* (*MMAR_0196*) gene was amplified from *M. marinum* genomic DNA using oligonucleotide primers orb95 (5′-TAGCCCACCAGCAGCCAATG-3′) and orb96 (5′-GCAGTCAGGCACCGTTGTCCGATGACGTCGAATCC-3′). The primers were designed to retain the first three codons of the *MMAR_0184* gene and the stop codon of the *esxA_2* gene. The p2NIL plasmid was amplified as described by Williams et al. (65). The p2NIL-ΔextESX-6 plasmid was generated using the FastCloning method, mixing the p2NIL PCR product with the upstream and downstream PCR products. The resulting p2NIL-ΔextESX-6 plasmid was confirmed by restriction digest and sequenced using oligonucleotide primers pNILFwdPst1 and p2NILRev. The pGOAL cassette was added as described by Williams et al. (65). The p2NIL-ΔextESX-6 suicide plasmid was UV treated and introduced into the WT strain by electroporation as described by Williams et al. (65). The final ΔextESX-6 strain was generated as described above. Loss of the *MMAR_0184-esxA_2* genes was screened by PCR analysis and verified by DNA sequencing of the PCR product with oligonucleotide primers orb127 (5′-ATTGCCACCGCAACC GAATG-3′) and orb128 (5′-CCGCGTAGTCCATTTCCAGC-3′).

DNA and protein alignments. *M. marinum* M strain DNA and protein sequences were obtained from MycoBrowser (60). Alignments were performed using Clustal Omega, and similarities were highlighted using BoxShade (69). Comparison of open reading frames with previously identified genes was performed by using the Basic Local Alignment Search Tool (BLAST) in the public National Center for Biotechnology Information databases and Clustal Omega.

Mycobacterial RNA extraction and cDNA synthesis. Cultures were grown in 7H9 broth and diluted to an OD_{600} of 0.8 in Sauton's defined broth supplemented with 0.01% Tween 80. Cells were collected after 48 h of growth. Total RNA from bacterial lysates was isolated using an RNeasy minikit (Qiagen, Hilden, Germany), according to the manufacturer's instructions. Bacterial lysates were generated by bead-beating cells resuspended in Qiagen RLT buffer supplemented with 1% β-mercaptoethanol as described previously (48).

For cDNA synthesis, 1 μg of total RNA was treated with DNase (Novagen, San Diego, CA) in a 10-μl reaction volume. EDTA (50 mM) was added to the DNase-treated RNA and incubated at 75°C for 10 min. Two microliters of DNase-treated RNA and 1 μl of 50 μM random hexamers were used for cDNA synthesis, which was performed as described in the manufacturer's protocol (Superscript II; Invitrogen).

qRT-PCR analysis. For qualitative RT-PCR (qRT-PCR) analysis, equal volumes of cDNA were used in each PCR. Expression of the *groEL2* gene was analyzed using oligonucleotide primers ors150 (5′-TGGA CAAGGTGGGCAACGAG-3′) and ors151 (5′-TGGAGCTGACCAGCAGGATG-3′). The experiment was performed on three independent biological replicates.

Quantification of *esxB* and *esxB_1* expression levels. The cDNA reaction mixture was diluted for qRT analysis and quantified using a NanoDrop spectrophotometer (ThermoScientific, Wilmington, DE). A standard curve was created by making dilutions of the WT sample. Twenty-microliter qRT-PCR mixtures were prepared using 2 μl (~460 to 560 ng) of the diluted cDNA, 500 nM primer, and SYBR Select Master mixture (Applied Biosystems, Carlsbad, CA). *esxB* and *esxB_1* were amplified with oligonucleotide primers ors148 (5′-ACCCAGATCGACCAGGTTGAG-3′) and ors149 (5′-GAAGCCCATTTGCGAGGACAG-3′). *esxA* was amplified using esxA5′ (5′-GGCAGCATCCAGCGCAATTC-3′) and esxA3′ (5′-GGTGGAGGACATTGCCTGAC-3′). *sigA* was amplified using oligonucleotide primers sigA-F and sigA-R (65). Samples were run on an Applied Biosystems 7500 Fast real-time PCR system. *esxB*, *esxB_1*, and *esxA* quantities were calculated relative to *sigA* levels. Biological replicates are indicated in the appropriate figure legends. Statistics were performed using GraphPad Prism, version 6.0. Statistical analysis was performed as described in the appropriate figure legends.

Hemolysis assays. The sheep red blood cell (sRBC) lysis assays were performed as previously described (67). Briefly, strains grown in 7H9 medium containing 0.1% Tween 80 to an OD_{600} between 2×10^8 and 6.5×10^8 bacteria were washed twice with phosphate-buffered saline (PBS) and incubated with defibrinated sRBCs (Hardy Diagnostics, Santa Maria, CA) as described previously (38, 67). OD_{405} readings were performed in technical triplicate using a SpectraMax M5 plate reader. The error bars represent standard deviations for technical triplicate readings. The data presented are representative of at least three biological replicates.

Protein preparation and analyses: ESX-1 secretion assay. ESX-1 protein secretion assays for *M. marinum* strains were performed exactly as described by Reyna et al. (67). Briefly, strains were grown in 25 ml of 7H9 broth containing 0.1% Tween 80 and then diluted to an OD_{600} of 0.8 in 50 ml of Sauton's defined broth with 0.01% Tween 80. The bacteria were grown for 48 h at 30°C, at which time the cells were collected by centrifugation. Whole-cell lysate and secreted protein fractions were generated as previously described by Kennedy et al. (41). Protein concentrations were determined using a MicroBCA protein assay (Thermo Scientific Pierce) according to the manufacturer's instructions with the following modification: plates were incubated for 30 min at 37°C. Ten to 15 micrograms of cell lysate and supernatant fractions was separated using a 4 to 20% Criterion or Mini-Protean TGX Tris-HCl precast polyacrylamide gel (Bio-Rad).

Proteins were analyzed by Western blot analysis using the following antibodies: RNA polymerase subunit β (RpoB) (1:5,000; ThermoScientific) and ESAT-6 (EsxA) (1:3,000 [HYB 076-08-02; Thermo Fisher, Waltham, MA]). The following reagents were obtained through BEI Resources, NIAID, NIH: NR-13801, polyclonal anti-*Mycobacterium tuberculosis* CFP-10 (gene Rv3874, 1:5,000), and NR-13807, polyclonal anti-*Mycobacterium tuberculosis* Mpt-32 (fibronectin attachment protein, or FAP; gene Rv1860, 1:5,000). Horseradish peroxidase (HRP)-conjugated goat anti-mouse and HRP-conjugated goat anti-rabbit antibodies were used (1:5,000; Bio-Rad Laboratories). All antibodies were resuspended in 5% milk in PBS with 0.1% Tween 20. Proteins were visualized using chemiluminescence (KPL, Gaithersburg, MD). Each blot is representative of three biological replicates.

Macrophage infection and RNA extraction. RAW 264.7 cells (ATCC TIB-71), a murine macrophage cell line, were maintained at 37°C and 5% CO_2 in Dulbecco's modified Eagle's medium (DMEM; Life Technologies, San Diego, CA) supplemented with 10% fetal bovine serum (FBS; HyClone Laboratories, Logan, UT). A total of 5×10^6 cells were seeded in a 24-well tissue culture (TC)-treated plate (Greiner Bio-one) overnight and infected at an MOI of 5. RNA extraction and DNase treatment were performed exactly as previously described (48).

IFN-β quantitative real-time PCR. Reaction mixtures for qRT-PCR analysis were prepared on ice using a Power SYBR Green RNA-to-C_T 1-Step kit (where C_T is threshold cycle) (Applied Biosystems), 500 nM each primer, and 40 ng of RNA. Oligonucleotide primers IFN-β-F and IFN-β-R were used to amplify IFN-β (13). Oligonucleotide primers β-actin-F and β-actin-R were used to analyze actin, which served as the reference gene (13). Samples were analyzed using an Applied Biosystems 7500 Fast real-time PCR system, with the same cycling parameters as described by Mba Medie et al. (48). A standard curve was generated by creating a dilution series of RNA collected from two WT infection wells. Each biological replicate was analyzed in technical duplicate. Statistical analysis was performed as described in the appropriate figure legends.

Amoeba cytotoxicity assay. A total of 5×10^5 cells of *Acanthamoeba castellanii* were seeded in a 24-well TC-treated plate (Greiner Bio-one). Amoebae were infected with *M. marinum* strains at an MOI of 10 for 2 h as described previously (48). Amoebae were stained at 24 h postinfection using ethidium homodimer 1 (EthD-1; Invitrogen/Molecular Probes, Carlsbad, CA) and imaged using an AxioObserver inverted microscope (Zeiss, Oberkochen, Germany). Two wells of amoebae were infected per strain. At least five images were taken randomly throughout each well. The EthD-1-stained cells were counted using ImageJ (70). Briefly, all images were analyzed under the default thresholding method with red as the thresholding color. The color space was selected as red-green-blue (RGB). Particles were then analyzed and counted by the ImageJ program as described previously (65). Statistical analysis was performed as described in the figure legends.

SUPPLEMENTAL MATERIAL

Supplemental material for this article may be found at https://doi.org/10.1128/JB.00726-17.

SUPPLEMENTAL FILE 1, PDF file, 0.5 MB.

ACKNOWLEDGMENTS

The Champion Laboratory is supported by the National Institute of Allergy and Infectious Diseases of the National Institutes of Health under award number R01 AI106872 to P.A.C. R.E.B. is supported by the National Science Foundation Graduate Research Fellowship Program under grant DGE-1313583. K.R.N. is supported by a Schmidt Fellowship through the University of Notre Dame.

Any opinions, findings, and conclusions or recommendations expressed in this material are those of the author(s) and do not necessarily reflect the views of the National Science Foundation or the National Institutes of Health.

We thank Matthew Champion for helpful discussion regarding the proteomic identification of EsxB_1.

We declare that the research was conducted in the absence of any commercial or financial relationships that could be construed as a potential conflict of interest.

Experiments were designed by R.E.B. and P.A.C. Experiments were performed by R.E.B., C.R.T., and K.R.N. R.E.B., C.R.T., and P.A.C. wrote the paper. All authors read and approved the manuscript.

REFERENCES

1. Feldman RA, Long MW, David HL. 1974. *Mycobacterium marinum*: a leisure-time pathogen. J Infect Dis 129:618–621. https://doi.org/10.1093/infdis/129.5.618.
2. Aronson JD. 1926. Spontaneous tuberculosis in salt water fish. J Infect Dis 39:315–320. https://doi.org/10.1093/infdis/39.4.315.
3. Guglielmetti L, Mougari F, Lopes A, Raskine L, Cambau E. 2015. Human infections due to nontuberculous mycobacteria: the infectious diseases and clinical microbiology specialists' point of view. Future Microbiol 10:1467–1483. https://doi.org/10.2217/fmb.15.64.
4. Aubry A, Mougari F, Reibel F, Cambau E. 2017. *Mycobacterium marinum*. Microbiol Spectr 5:4. https://doi.org/10.1128/microbiolspec.TNMI7-0038-2016.
5. Koch R. 1952. Tuberculosis etiology. Dtsch Gesundheitsw 7:457–465. (Undetermined language.)
6. Lienard J, Carlsson F. 2017. Murine *Mycobacterium marinum* Infection as a Model for Tuberculosis. Methods Mol Biol 1535:301–315. https://doi.org/10.1007/978-1-4939-6673-8_20.
7. Hsu T, Hingley-Wilson SM, Chen B, Chen M, Dai AZ, Morin PM, Marks CB, Padiyar J, Goulding C, Gingery M, Eisenberg D, Russell RG, Derrick SC, Collins FM, Morris SL, King CH, Jacobs WR, Jr. 2003. The primary mechanism of attenuation of bacillus Calmette-Guerin is a loss of secreted lytic function required for invasion of lung interstitial tissue. Proc Natl Acad Sci U S A 100:12420–12425. https://doi.org/10.1073/pnas.1635213100.
8. Stanley SA, Raghavan S, Hwang WW, Cox JS. 2003. Acute infection and macrophage subversion by *Mycobacterium tuberculosis* require a specialized secretion system. Proc Natl Acad Sci U S A 100:13001–13006. https://doi.org/10.1073/pnas.2235593100.
9. Guinn KM, Hickey MJ, Mathur SK, Zakel KL, Grotzke JE, Lewinsohn DM, Smith S, Sherman DR. 2004. Individual RD1-region genes are required for export of ESAT-6/CFP-10 and for virulence of *Mycobacterium tuberculosis*. Mol Microbiol 51:359–370. https://doi.org/10.1046/j.1365-2958.2003.03844.x.
10. Abdallah AM, Verboom T, Hannes F, Safi M, Strong M, Eisenberg D, Musters RJ, Vandenbroucke-Grauls CM, Appelmelk BJ, Luirink J, Bitter W. 2006. A specific secretion system mediates PPE41 transport in pathogenic mycobacteria. Mol Microbiol 62:667–679. https://doi.org/10.1111/j.1365-2958.2006.05409.x.
11. Mehra A, Zahra A, Thompson V, Sirisaengtaksin N, Wells A, Porto M, Koster S, Penberthy K, Kubota Y, Dricot A, Rogan D, Vidal M, Hill DE, Bean AJ, Philips JA. 2013. *Mycobacterium tuberculosis* type VII secreted effector EsxH targets host ESCRT to impair trafficking. PLoS Pathog 9:e1003734. https://doi.org/10.1371/journal.ppat.1003734.
12. Volkman HE, Clay H, Beery D, Chang JC, Sherman DR, Ramakrishnan L. 2004. Tuberculous granuloma formation is enhanced by a mycobacterium virulence determinant. PLoS Biol 2:e367. https://doi.org/10.1371/journal.pbio.0020367.
13. Stanley SA, Johndrow JE, Manzanillo P, Cox JS. 2007. The Type I IFN response to infection with *Mycobacterium tuberculosis* requires ESX-1-mediated secretion and contributes to pathogenesis. J Immunol 178:3143–3152. https://doi.org/10.4049/jimmunol.178.5.3143.
14. Simeone R, Bobard A, Lippmann J, Bitter W, Majlessi L, Brosch R, Enninga J. 2012. Phagosomal rupture by *Mycobacterium tuberculosis* results in toxicity and host cell death. PLoS Pathog 8:e1002507. https://doi.org/10.1371/journal.ppat.1002507.
15. Manzanillo PS, Shiloh MU, Portnoy DA, Cox JS. 2012. *Mycobacterium tuberculosis* activates the DNA-dependent cytosolic surveillance pathway within macrophages. Cell Host Microbe 11:469–480. https://doi.org/10.1016/j.chom.2012.03.007.
16. Watson RO, Manzanillo PS, Cox JS. 2012. Extracellular *M. tuberculosis* DNA targets bacteria for autophagy by activating the host DNA-sensing pathway. Cell 150:803–815. https://doi.org/10.1016/j.cell.2012.06.040.
17. van der Wel N, Hava D, Houben D, Fluitsma D, van Zon M, Pierson J, Brenner M, Peters PJ. 2007. *M. tuberculosis* and *M. leprae* translocate from the phagolysosome to the cytosol in myeloid cells. Cell 129:1287–1298. https://doi.org/10.1016/j.cell.2007.05.059.
18. Stamm LM, Morisaki JH, Gao LY, Jeng RL, McDonald KL, Roth R, Takeshita S, Heuser J, Welch MD, Brown EJ. 2003. *Mycobacterium marinum* escapes from phagosomes and is propelled by actin-based motility. J Exp Med 198:1361–1368. https://doi.org/10.1084/jem.20031072.
19. Lienard J, Movert E, Valfridsson C, Sturegard E, Carlsson F. 2016. ESX-1 exploits type I IFN-signalling to promote a regulatory macrophage phenotype refractory to IFNγ-mediated autophagy and growth restriction of intracellular mycobacteria. Cell Microbiol 18:1471–1485. https://doi.org/10.1111/cmi.12594.
20. Conrad WH, Osman MM, Shanahan JK, Chu F, Takaki KK, Cameron J, Hopkinson-Woolley D, Brosch R, Ramakrishnan L. 2017. Mycobacterial ESX-1 secretion system mediates host cell lysis through bacterium contact-dependent gross membrane disruptions. Proc Natl Acad Sci U S A 114:1371–1376. https://doi.org/10.1073/pnas.1620133114.
21. Gey Van Pittius NC, Gamieldien J, Hide W, Brown GD, Siezen RJ, Beyers AD. 2001. The ESAT-6 gene cluster of *Mycobacterium tuberculosis* and other high G+C Gram-positive bacteria. Genome Biol 2:RESEARCH0044. https://doi.org/10.1186/gb-2001-2-10-research0044.
22. Pallen MJ. 2002. The ESAT-6/WXG100 superfamily – and a new Gram-positive secretion system? Trends Microbiol 10:209–212. https://doi.org/10.1016/S0966-842X(02)02345-4.
23. Berthet FX, Rasmussen PB, Rosenkrands I, Andersen P, Gicquel B. 1998. A *Mycobacterium tuberculosis* operon encoding ESAT-6 and a novel low-molecular-mass culture filtrate protein (CFP-10). Microbiology 144:3195–3203. https://doi.org/10.1099/00221287-144-11-3195.
24. Renshaw PS, Panagiotidou P, Whelan A, Gordon SV, Hewinson RG, Williamson RA, Carr MD. 2002. Conclusive evidence that the major T-cell antigens of the *Mycobacterium tuberculosis* complex ESAT-6 and CFP-10 form a tight, 1:1 complex and characterization of the structural proper-

ties of ESAT-6, CFP-10, and the ESAT-6*CFP-10 complex. Implications for pathogenesis and virulence. J Biol Chem 277:21598–21603.
25. Renshaw PS, Lightbody KL, Veverka V, Muskett FW, Kelly G, Frenkiel TA, Gordon SV, Hewinson RG, Burke B, Norman J, Williamson RA, Carr MD. 2005. Structure and function of the complex formed by the tuberculosis virulence factors CFP-10 and ESAT-6. EMBO J 24:2491–2498. https://doi.org/10.1038/sj.emboj.7600732.
26. Champion PA, Stanley SA, Champion MM, Brown EJ, Cox JS. 2006. C-terminal signal sequence promotes virulence factor secretion in *Mycobacterium tuberculosis*. Science 313:1632–1636. https://doi.org/10.1126/science.1131167.
27. Champion MM, Williams EA, Pinapati RS, Champion PA. 2014. Correlation of phenotypic profiles using targeted proteomics identifies mycobacterial Esx-1 substrates. J Proteome Res 13:5151–5164. https://doi.org/10.1021/pr500484w.
28. Rosenberg OS, Dovala D, Li X, Connolly L, Bendebury A, Finer-Moore J, Holton J, Cheng Y, Stroud RM, Cox JS. 2015. Substrates control multimerization and activation of the multi-domain ATPase motor of type VII secretion. Cell 161:501–512. https://doi.org/10.1016/j.cell.2015.03.040.
29. MacGurn JA, Raghavan S, Stanley SA, Cox JS. 2005. A non-RD1 gene cluster is required for Snm secretion in *Mycobacterium tuberculosis*. Mol Microbiol 57:1653–1663. https://doi.org/10.1111/j.1365-2958.2005.04800.x.
30. McLaughlin B, Chon JS, MacGurn JA, Carlsson F, Cheng TL, Cox JS, Brown EJ. 2007. A mycobacterium ESX-1-secreted virulence factor with unique requirements for export. PLoS Pathog 3:e105. https://doi.org/10.1371/journal.ppat.0030105.
31. Fortune SM, Jaeger A, Sarracino DA, Chase MR, Sassetti CM, Sherman DR, Bloom BR, Rubin EJ. 2005. Mutually dependent secretion of proteins required for mycobacterial virulence. Proc Natl Acad Sci U S A 102:10676–10681. https://doi.org/10.1073/pnas.0504922102.
32. Gey van Pittius NC, Sampson SL, Lee H, Kim Y, van Helden PD, Warren RM. 2006. Evolution and expansion of the *Mycobacterium tuberculosis* PE and PPE multigene families and their association with the duplication of the ESAT-6 (*esx*) gene cluster regions. BMC Evol Biol 6:95. https://doi.org/10.1186/1471-2148-6-95.
33. Fishbein S, van Wyk N, Warren RM, Sampson SL. 2015. Phylogeny to function: PE/PPE protein evolution and impact on *Mycobacterium tuberculosis* pathogenicity. Mol Microbiol 96:901–916. https://doi.org/10.1111/mmi.12981.
34. Shah S, Cannon JR, Fenselau C, Briken V. 2015. A duplicated ESAT-6 region of ESX-5 is involved in protein export and virulence of mycobacteria. Infect Immun 83:4349–4361. https://doi.org/10.1128/IAI.00827-15.
35. Stinear TP, Seemann T, Harrison PF, Jenkin GA, Davies JK, Johnson PD, Abdellah Z, Arrowsmith C, Chillingworth T, Churcher C, Clarke K, Cronin A, Davis P, Goodhead I, Holroyd N, Jagels K, Lord A, Moule S, Mungall K, Norbertczak H, Quail MA, Rabbinowitsch E, Walker D, White B, Whitehead S, Small PL, Brosch R, Ramakrishnan L, Fischbach MA, Parkhill J, Cole ST. 2008. Insights from the complete genome sequence of *Mycobacterium marinum* on the evolution of *Mycobacterium tuberculosis*. Genome Res 18:729–741. https://doi.org/10.1101/gr.075069.107.
36. Daleke MH, Ummels R, Bawono P, Heringa J, Vandenbroucke-Grauls CM, Luirink J, Bitter W. 2012. General secretion signal for the mycobacterial type VII secretion pathway. Proc Natl Acad Sci U S A 109:11342–11347. https://doi.org/10.1073/pnas.1119453109.
37. King CH, Mundayoor S, Crawford JT, Shinnick TM. 1993. Expression of contact-dependent cytolytic activity by *Mycobacterium tuberculosis* and isolation of the genomic locus that encodes the activity. Infect Immun 61:2708–2712.
38. Gao LY, Guo S, McLaughlin B, Morisaki H, Engel JN, Brown EJ. 2004. A mycobacterial virulence gene cluster extending RD1 is required for cytolysis, bacterial spreading and ESAT-6 secretion. Mol Microbiol 53:1677–1693. https://doi.org/10.1111/j.1365-2958.2004.04261.x.
39. Abdallah AM, Bestebroer J, Savage ND, de Punder K, van Zon M, Wilson L, Korbee CJ, van der Sar AM, Ottenhoff TH, van der Wel NN, Bitter W, Peters PJ. 2011. Mycobacterial secretion systems ESX-1 and ESX-5 play distinct roles in host cell death and inflammasome activation. J Immunol 187:4744–4753. https://doi.org/10.4049/jimmunol.1101457.
40. Kennedy GM, Morisaki JH, Champion PA. 2012. Conserved mechanisms of *Mycobacterium marinum* pathogenesis within the environmental amoeba, *Acanthamoeba castellanii*. Appl Environ Microbiol 8:2049–2052. https://doi.org/10.1128/AEM.06965-11.
41. Kennedy GM, Hooley GC, Champion MM, Medie FM, Champion PA. 2014. A novel ESX-1 locus reveals that surface associated ESX-1 substrates mediate virulence in *Mycobacterium marinum*. J Bacteriol 196:1877–1888. https://doi.org/10.1128/JB.01502-14.
42. Champion PA, Champion MM, Manzanillo P, Cox JS. 2009. ESX-1 secreted virulence factors are recognized by multiple cytosolic AAA ATPases in pathogenic mycobacteria. Mol Microbiol 73:950–962. https://doi.org/10.1111/j.1365-2958.2009.06821.x.
43. Champion PA. 2013. Disconnecting in vitro ESX-1 secretion from mycobacterial virulence. J Bacteriol 195:5418–5420. https://doi.org/10.1128/JB.01145-13.
44. Siegrist MS, Steigedal M, Ahmad R, Mehra A, Dragset MS, Schuster BM, Phillips JA, Carr SA, Rubin EJ. 2014. Mycobacterial ESX-3 requires multiple components for iron acquisition. mBio 5:e01073-14. https://doi.org/10.1128/mBio.01073-14.
45. Chen JM, Zhang M, Rybniker J, Basterra L, Dhar N, Tischler AD, Pojer F, Cole ST. 2013. Phenotypic profiling of *Mycobacterium tuberculosis* EspA point-mutants reveals blockage of ESAT-6 and CFP-10 secretion in vitro does not always correlate with attenuation of virulence. J Bacteriol 195:5421–5430. https://doi.org/10.1128/JB.00967-13.
46. Rybniker J, Chen JM, Sala C, Hartkoorn RC, Vocat A, Benjak A, Boy-Rottger S, Zhang M, Szekely R, Greff Z, Orfi L, Szabadkai I, Pato J, Keri G, Cole ST. 2014. Anticytolytic screen identifies inhibitors of mycobacterial virulence protein secretion. Cell Host Microbe 16:538–548. https://doi.org/10.1016/j.chom.2014.09.008.
47. Houben D, Demangel C, van Ingen J, Perez J, Baldeon L, Abdallah AM, Caleechurn L, Bottai D, van Zon M, de Punder K, van der Laan T, Kant A, Bossers-de Vries R, Willemsen P, Bitter W, van Soolingen D, Brosch R, van der Wel N, Peters PJ. 2012. ESX-1-mediated translocation to the cytosol controls virulence of mycobacteria. Cell Microbiol 14:1287–1298. https://doi.org/10.1111/j.1462-5822.2012.01799.x.
48. Mba Medie F, Champion MM, Williams EA, Champion PAD. 2014. Homeostasis of N-α-terminal acetylation of EsxA correlates with virulence in *Mycobacterium marinum*. Infect Immun 82:4572–4586. https://doi.org/10.1128/IAI.02153-14.
49. Chen JM, Boy-Rottger S, Dhar N, Sweeney N, Buxton RS, Pojer F, Rosenkrands I, Cole ST. 2012. EspD is critical for the virulence-mediating ESX-1 secretion system in *Mycobacterium tuberculosis*. J Bacteriol 194:884–893. https://doi.org/10.1128/JB.06417-11.
50. Weerdenburg EM, Abdallah AM, Rangkuti F, Abd El Ghany M, Otto TD, Adroub SA, Molenaar D, Ummels R, Ter Veen K, van Stempvoort G, van der Sar AM, Ali S, Langridge GC, Thomson NR, Pain A, Bitter W. 2015. Genome-wide transposon mutagenesis indicates that *Mycobacterium marinum* customizes its virulence mechanisms for survival and replication in different hosts. Infect Immun 83:1778–1788. https://doi.org/10.1128/IAI.03050-14.
51. Tobias NJ, Doig KD, Medema MH, Chen H, Haring V, Moore R, Seemann T, Stinear TP. 2013. Complete genome sequence of the frog pathogen *Mycobacterium ulcerans* ecovar Liflandii. J Bacteriol 195:556–564. https://doi.org/10.1128/JB.02132-12.
52. Stinear TP, Seemann T, Pidot S, Frigui W, Reysset G, Garnier T, Meurice G, Simon D, Bouchier C, Ma L, Tichit M, Porter JL, Ryan J, Johnson PD, Davies JK, Jenkin GA, Small PL, Jones LM, Tekaia F, Laval F, Daffe M, Parkhill J, Cole ST. 2007. Reductive evolution and niche adaptation inferred from the genome of *Mycobacterium ulcerans*, the causative agent of Buruli ulcer. Genome Res 17:192–200. https://doi.org/10.1101/gr.5942807.
53. Doig KD, Holt KE, Fyfe JA, Lavender CJ, Eddyani M, Portaels F, Yeboah-Manu D, Pluschke G, Seemann T, Stinear TP. 2012. On the origin of *Mycobacterium ulcerans*, the causative agent of Buruli ulcer. BMC Genomics 13:258. https://doi.org/10.1186/1471-2164-13-258.
54. Sani M, Houben EN, Geurtsen J, Pierson J, de Punder K, van Zon M, Wever B, Piersma SR, Jimenez CR, Daffe M, Appelmelk BJ, Bitter W, van der Wel N, Peters PJ. 2010. Direct visualization by cryo-EM of the mycobacterial capsular layer: a labile structure containing ESX-1-secreted proteins. PLoS Pathog 6:e1000794. https://doi.org/10.1371/journal.ppat.1000794.
55. Phan TH, Ummels R, Bitter W, Houben EN. 2017. Identification of a substrate domain that determines system specificity in mycobacterial type VII secretion systems. Sci Rep 7:42704. https://doi.org/10.1038/srep42704.
56. Duprey A, Nasser W, Leonard S, Brochier-Armanet C, Reverchon S. 2016. Transcriptional start site turnover in the evolution of bacterial paralogous genes—the pelE-pelD virulence genes in Dickeya. FEBS J 283:4192–4207. https://doi.org/10.1111/febs.13921.
57. Bosserman RE, Nguyen TT, Sanchez KG, Chirakos AE, Ferrell MJ, Thomp-

son CR, Champion MM, Abramovitch RB, Champion PA. 2017. WhiB6 regulation of ESX-1 gene expression is controlled by a negative feedback loop in *Mycobacterium marinum*. Proc Natl Acad Sci U S A 114: E10772–E10781. https://doi.org/10.1073/pnas.1710167114.
58. Carlsson F, Joshi SA, Rangell L, Brown EJ. 2009. Polar localization of virulence-related Esx-1 secretion in mycobacteria. PLoS Pathog 5:e1000285. https://doi.org/10.1371/journal.ppat.1000285.
59. Bottai D, Di Luca M, Majlessi L, Frigui W, Simeone R, Sayes F, Bitter W, Brennan MJ, Leclerc C, Batoni G, Campa M, Brosch R, Esin S. 2012. Disruption of the ESX-5 system of *Mycobacterium tuberculosis* causes loss of PPE protein secretion, reduction of cell wall integrity and strong attenuation. Mol Microbiol 83:1195–1209. https://doi.org/10.1111/j.1365-2958.2012.08001.x.
60. Kapopoulou A, Lew JM, Cole ST. 2011. The MycoBrowser portal: a comprehensive and manually annotated resource for mycobacterial genomes. Tuberculosis (Edinb) 91:8–13. https://doi.org/10.1016/j.tube.2010.09.006.
61. Solomon JM, Leung GS, Isberg RR. 2003. Intracellular replication of *Mycobacterium marinum* within *Dictyostelium discoideum:* efficient replication in the absence of host coronin. Infect Immun 71:3578–3586. https://doi.org/10.1128/IAI.71.6.3578-3586.2003.
62. Bitter W, Houben EN, Bottai D, Brodin P, Brown EJ, Cox JS, Derbyshire K, Fortune SM, Gao LY, Liu J, Gey van Pittius NC, Pym AS, Rubin EJ, Sherman DR, Cole ST, Brosch R. 2009. Systematic genetic nomenclature for type VII secretion systems. PLoS Pathog 5:e1000507. https://doi.org/10.1371/journal.ppat.1000507.
63. Gao LY, Groger R, Cox JS, Beverley SM, Lawson EH, Brown EJ. 2003. Transposon mutagenesis of *Mycobacterium marinum* identifies a locus linking pigmentation and intracellular survival. Infect Immun 71: 922–929. https://doi.org/10.1128/IAI.71.2.922-929.2003.
64. Li C, Wen A, Shen B, Lu J, Huang Y, Chang Y. 2011. FastCloning: a highly simplified, purification-free, sequence- and ligation-independent PCR cloning method. BMC Biotechnol 11:92. https://doi.org/10.1186/1472-6750-11-92.
65. Williams EA, Mba Medie F, Bosserman RE, Johnson BK, Reyna C, Ferrell MJ, Champion MM, Abramovitch RB, Champion PA. 2017. A nonsense mutation in *Mycobacterium marinum* that is suppressible by a novel mechanism. Infect Immun 85:e00653-16. https://doi.org/10.1128/IAI.00653-16.
66. George KM, Yuan Y, Sherman DR, Barry CE, III. 1995. The biosynthesis of cyclopropanated mycolic acids in *Mycobacterium tuberculosis*. Identification and functional analysis of CMAS-2. J Biol Chem 270:27292–27298.
67. Reyna C, Mba Medie F, Champion MM, Champion PA. 2016. Rational engineering of a virulence gene from *Mycobacterium tuberculosis* facilitates proteomic analysis of a natural protein N terminus. Sci Rep 6:33265. https://doi.org/10.1038/srep33265.
68. Parish T, Stoker NG. 2000. Use of a flexible cassette method to generate a double unmarked Mycobacterium tuberculosis tlyA plcABC mutant by gene replacement. Microbiology 146:1969–1975. https://doi.org/10.1099/00221287-146-8-1969.
69. Sievers F, Wilm A, Dineen D, Gibson TJ, Karplus K, Li W, Lopez R, McWilliam H, Remmert M, Soding J, Thompson JD, Higgins DG. 2011. Fast, scalable generation of high-quality protein multiple sequence alignments using Clustal Omega. Mol Syst Biol 7:539. https://doi.org/10.1038/msb.2011.75.
70. Schneider CA, Rasband WS, Eliceiri KW. 2012. NIH Image to ImageJ: 25 years of image analysis. Nat Methods 9:671–675. https://doi.org/10.1038/nmeth.2089.